Analysis of Precision Deburring Using a Laser -An Experimental Study and FEM Simulation

Seoung Hwan Lee*
Department of Mechanical Engineering Hanyang University

The purpose of this study is to develop an effective method for automated deburring of precision components. A high power laser is proposed as a deburring tool for complex part edges and burrs. For the laser experiments, rectangular-shaped carbon steel and stainless steel machined specimens with burr along one side were prepared. A 1500 Watt CO_2 laser was used to remove burrs on the workpieces. The prediction of the heat affected zone (HAZ) and cutting profile of laser-deburred parts using finite element method is presented and compared with the experimental results. This study shows that the finite element method (FEM) analysis can effectively predict the thermal affected zone of the material and that the technique can be applied to precision components.

Key Words: Burr, Precision Deburring, High Power Laser, HAZ, FEM

1. Introduction

Burrs have been defined as undesirable projections of material beyond the edge of the workpiece due to plastic deformation during machining (Ko, 1993). Burrs cause many problems in inspection, assembly, and manufacturing automation of precision components. Especially, deburring and edge finishing of precision parts may contribute as much as 30% of the part cost as well as cause additional dimensional errors (Gillespie, 1979). Consequently, the automation of the deburring process, along with effective burr-removing techniques, has become a prime objective as part of efforts to automate the entire manufacturing system.

Recent developments in automated deburring include several process-oriented techniques such as tumbling, electrochemical deburring, abrasive jet machining, water jet machining and vibratory finishing. However, these methods have certain limitations in some applications. Tumbling or vibratory finishing removes material from all surfaces of the part instead of the confined edges of the workpiece (De Litzia, 1986, Kittedge, 1989). Tumbling and abrasive jet machining have geometric limitations in applications which prevent them from deburring internal portions of the part (Alwerfalli, 1975). Some electrochemical deburring methods need post processing to remove unwanted residuals (Sonego, 1988). Abrasive or jet machining is most effective only on thin section or light weight burrs composed of brittle materials (Roberts, 1985). Sensing-oriented deburring approaches also have been tried. Acoustic emission (Manz, 1990) or force signal (Stepian, 1987) is used as a closed loop feedback in a computer controlled deburring algorithm. As an implementation of AE sensing to actual deburring, Masaki and Dornfeld (1987) used a cutting/deburring tool to remove the burr by chamfering. Their work was done either open loop or as part of a closed loop feedback on a computer controlled deburring machine with sensor feedback. However, the contact between the tool and the workpiece can cause problems when precision is required.

* **E-mail** : sunglee@email. hanyang. ac. kr
TEL : +82-345-400-5288 **FAX** : +82-345-406-5550
Department of Mechanical Engineering, Hanyang University, 1271, Sal-dong, Ansan, Kyunggi-do 425-791, Korea. (Manuscript **Received** January 25, 1999; **Revised** August 9, 1999)

Since the above methods always generate mechanical contact between the tool and the workpiece, they may have additional disturbances such as material damage, tool wear and vibrational effects. Also, with conventional methods, it is very hard to get robust sensor feedback due to the contact and the irregularity of edge profiles. In recent years, a thermal process, laser machining, has been successfully introduced in various operations such as cutting, scribing (Chryssolouris, 1990) along with surface treatment, drilling (Wei & Chiou, 1988, Wei & Ho, 1990), and sheet metal forming (Geiger, 1988). Since laser machining is a tool-free, non-contact process, it can provide a very flexible machining operation as long as the thermal properties of the material are adequate and sufficient process control can be acquired. Today, laser systems are powerful (up to 45 kW), accurate (submicron), compact, and can be easily automated (mounted directly on a robot arm) (Cai, 1996). All the advantages of laser technology can be utilized for laser deburring, as it is essentially an application of laser cutting to remove burrs from part edges.

This study was to investigate the applicability and viability of laser machining in automated precision deburring. Both experimental work and FEM simulation were conducted in the research.

2. Laser Deburring

2.1 Review of laser cutting and deburring

The results of research in laser machining or laser welding can be found in the literature. As laser machining is a thermal process, many researchers also have performed thermal analyses to investigate the heat source (laser) or the thermal effects including the heat affected zone of the laser on a workpiece. An early pioneer, Rosenthal (1941) gave an analytical solution for the temperature field in a workpiece which was subjected to a moving heat source like a laser beam. This solution assumes constant thermal properties and does not account for the removal of material as it melts. Meherabian and Hsu (1978) conducted a three dimensional heat flow analysis concerned with the rapid melting and solidification of a surface subjected to a moving heat source. They compared their model predictions with experimental observations qualitatively. Glass et al. (1977) developed a numerical model to achieve proper material removal by the laser, to account for the energy lost through the kerf and to predict the temperature field in the material adjacent to the cut (HAZ). The predictions obtained from the model were compared with experimental cutting data. In this model the effects of parameters like cutting speed and power were related to the size of the cut and the extent of the HAZ. Masumoto and Shinoda (1990) investigated the corrosion zone formed in AISI 304 stainless steel welded joints. They used surface laser treatment to achieve extremely high heating and quenching rates which dissolves the already existing carbides in the HAZ into solution. Nakao and Nishimoto (1986) also studied austenitic stainless steels which were sensitized in the HAZ due to the depletion of chromium. They successfully demonstrated the use of laser to desensitize the HAZ. However they did not address the issues of the extent of heat affected zones due to the laser machining itself.

Other researchers conducted the thermal analysis in laser machining of various materials. Paek and Gagliano (1972) developed a model that used a continuous distributed and moving heat source to describe the temperature profile and thermal stress propagation for laser drilled holes. They, however, assumed that the thermal and mechanical properties of the material are independent of temperature and there are no heat losses through the bounding surfaces. Katayama and Matsunawa (1985) observed solidification microstructures of continuous CO_2 laser welds in commercial austenitic stainless steels of type 310S and 304. Their study involves the comparison between microstructural changes in the HAZ for pulsed laser and continuous laser. They have not dealt with the extent of the HAZ on the microstructures which is important in defining the HAZ of austenitic stainless steels.

The laser machined part geometry is of importance. There has been a lot of work done to predict the laser cutting geometry by analyzing

the effects of laser machining parameters such as beam energy, heat conduction and plasma, etc. Rajaram and Coyle (1983) developed a numerical model to study laser material processing. Their particular attention was, however, focused on predicting the depths and the widths of the fusion zone. Cline and Anthony (1977) performed a thermal analysis for laser heating and melting of materials. They related experimental temperature distribution, cooling rate distribution and depth of melting to the laser spot size, velocity and power level. They analyzed the thermal distribution from a moving Gaussian source over a large range of conditions from simple heat treating to deep penetration welding. However, their analysis was limited to laser drilling (one dimensional) only. Petring et al. (1988) formulated a laser cutting front geometry based on a power balance between surface absorption, material melting and heating, and conduction. They used a simplified cutting front by assuming a constant kerf width equal to the beam diameter. The heat conduction loss in laser cutting of metal was studied by Shulz et al. (1991). In this model, the generated cutting kerf was solved using numerical calculation. Also, temperature dependent material properties were taken into account in this model. Model estimation showed reasonable correlation with experiments even though the model greatly simplified the melting front.

Except for a few patented works, there has been little concentration on laser deburring in the research literature. Lange et al. (1992) mentioned the existence of burrs after laser machining of sheet metals, but that was only a small portion of a description in which the quality of the entire cut face of the metal sheets after laser cutting was explained. The difficulties to apply existing laser cutting models to laser deburring are:

1. There are few available analytical closed form solutions which can effectively describe the complicated thermo-mechanical problems with large deformation and steep temperature gradients. In fact, most laser cutting models assume a simplified and symmetric cutting geometry, which is not applicable to laser deburring (see, Fig. 2) because of the heat convection and radiation at the deburring boundary.

2. Most of the previous research is concentrated on either prediction of cutting geometry or investigation of the HAZ, but not both. As both the cutting geometry and material property changes near the cutting surface are important in deburring, a special model for laser deburring is needed.

With the advent of various numerical solution techniques including finite element methods (Pertring et al., 1988, Shulz et al., 1991), many investigators successfully studied the temperature and stress fields in thermal machining or predicted the cutting geometry through numerical analysis. In this study, simulation analysis using the FEM was selected to model the physical phenomena in laser deburring. The FEM analysis can provide a preliminary guide line before performing the actual laser deburring experiments. FEM is also a tool for the analysis of the effects of experimental parameters, as it can predict important features such as cutting dimensions and the size of the HAZ. The result from FEM simulation was compared to experimental results.

2.2 Deburring experiment

Figure 1 shows the experimental setup for laser deburring. A 1500W CO_2 laser, with a three dimensional positioning system and a coaxial gas jet support was used for the laser experiments. Figure 2(a) shows a schematic of the laser deburring experiment used in this study. For the experiment, rectangular-shaped carbon steel (AISI 1045) and stainless steel (SS304) machined specimens with burrs along one side were used. With the laser equipment properly positioned, a laser beam is impinged tangentially (y-direction), i. e., normal to the burr height (x) direction (Fig. 2 (b)), to the workpiece and the beam accurately melts away the burrs on the specimen as the specimen is moving at a given feed rate of 0.5 mm/sec. to 2.5 mm/sec. Table 1 shows the typical cutting profiles obtained from the laser deburring experiment.

Figure 3 shows the SEM micrographs for the a comparison between laser deburring and mechanical deburring. Two stainless steel workpieces

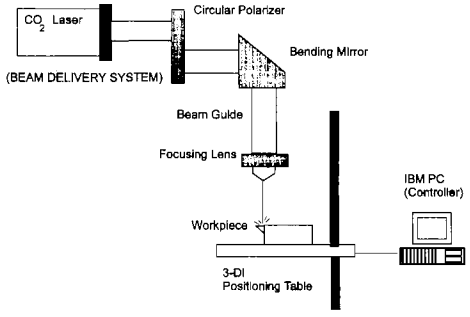

Fig. 1 Experimental setup

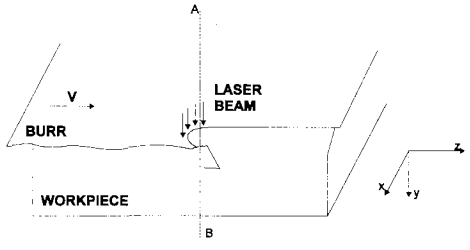

(a)

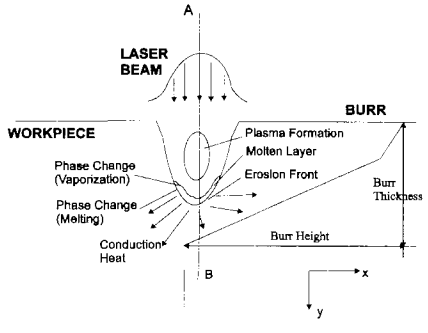

(b)

Fig. 2 Laser deburring

with similar burr shapes (upper picture) were deburred manually and with the laser (beam impinged from top to bottom direction), respectively. Also, Fig. 4 shows a specimen with burr and the laser cut profile of the specimen after deburring for Carbon Steel 1045.

There are several advantages of using lasers for deburring over conventional (mechanical) deburring method. First, as shown in Table 1, a smaller amount of material will be removed by using the laser. In fact, for the carbon steel case, a very narrow laser cutting kerf was observed, as higher aspect ratios (cut depth/cut width) of up to 10 to 1, are obtainable (AWS, 1991) using the laser. Second, maintaining constant depth of cut, which is an important factor for the controllability of deburring processes, is much easier in laser deburring than in mechanical deburring because non-uniform contact occurs during mechanical deburring, especially when the burrs have some irregularity. Third, compared to other thermal processes, the heat input in laser machining is close to the minimum required to melt the workpiece material; thus, metallurgical effects in HAZ as well as the size of the HAZ itself are reduced, and heat-induced distortion is minimized (AWS, 1991).

2.3 Heat affected zone

The HAZ is the region near the cutting area which is transformed by the high temperature of the process. Inside the HAZ, grain size change and subsequent material property changes are expected (Schey, 1987). For example, a part of the heated zone of stainless steel 304 -in which no phase transformation will occur- may become highly susceptible to corrosion due to carbide-precipitation along the grain boundaries when heated to a temperature within a certain range and cooled at a slow enough rate. Also, steels may experience residual stress after rapid heating and cooling in addition to the change in grain size. In both cases, there are material property changes inside the HAZ, which are detrimental, particularly with respect to wear resistance. Though the size and characteristics of the HAZ are different for different materials, Fig. 5(a) shows a possible phase diagram and temperature profile in a workpiece due to welding for describing the HAZ for carbon steel 1045, which is one of the materials used in the experiments. For the carbon steel, the material near the heated zone will be experiencing a phase transformation (austenite to ferrite or martensite) at an elevated transformation temperature (Kuilboer et al., 1994) due to the fast cooling rate during laser machining. In both materials, recrystallization due to the previous cold working (burr making) is expected. Even inside the zone, the material will have different grain sizes depending on the

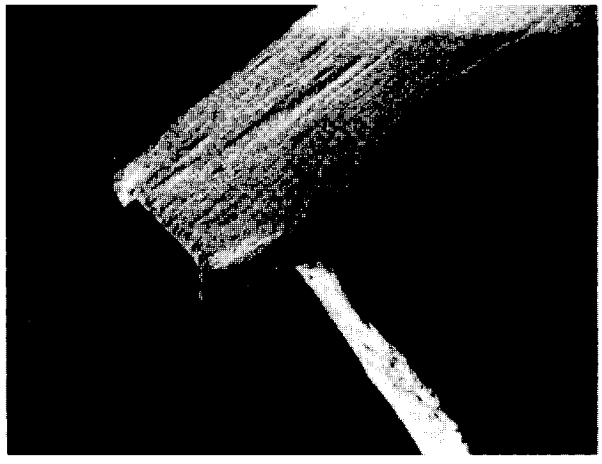

Burr Specimen (Burr Height = 1mm)

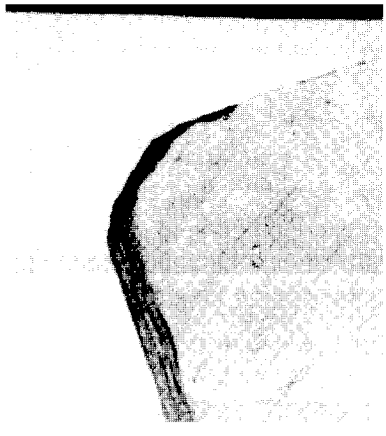

Cutting Profile for SS304
(Mechanical Deburring)

Cutting Profile for SS304
(Laser Power = 300W, Wir Jet)

Fig. 3 Cutting profiles for SS304 (X30)

Burr Specimen
(Burr Height = 0.5mm)

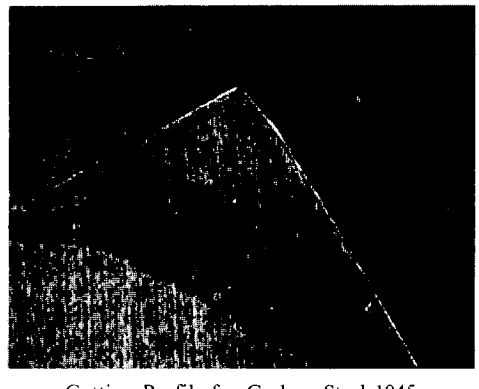

Cutting Profile for Carbon Steel 1045
(Laser Power = 400W, Air Jet)

Fig. 4 Cutting profile for carbon steel (X30)

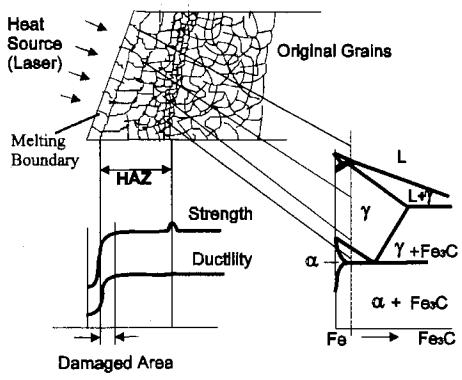

(a)

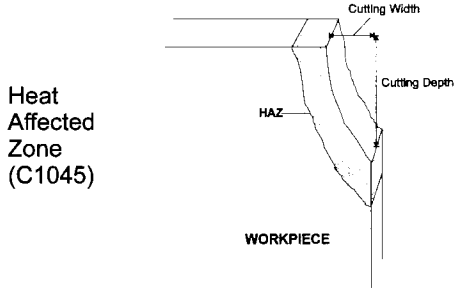

(b)

Fig. 5 (a) Phase diagram for carbon steel
(b) Heat affected zone (carbon steel)

maximum temperature and cooling rate at that location. For instance, the material near the heat source (laser) will have a slower cooling rate. Thus, the grain size will be relatively coarse. The material near the zone (outside) boundary has a faster cooling rate and finer grain size. Ideally, the HAZ should be minimized to prevent damage or change in material properties to the parent material. Therefore, a main objective of this research will be the prediction and minimization or control of the HAZ.

In the carbon steel experiments, a gray-colored surface zone was observed near the cut area after laser deburring (Fig. 5(b)). The deburred workpiece was sectioned and polished then etched with a 37 volume % HCl solution. The etching time was in the range of 0.5-1 hours (until the disappearance of bubbles, which is the characteristics of etching of iron). The etched surfaces were subsequently viewed under the microscope to reveal any changes in the microstructure of the material inside the colored zone. Grain size refinement was observed (Fig. 6(a)) inside the region and this is defined as the HAZ for carbon steel in laser deburring. Inside the HAZ, very coarse grains found at the melt boundary gradually change to finer ones until, at the edge of the HAZ, only partial recrystallization is evident. If cooling rate is fast at the edge of the HAZ, the material in that region will be converted into martensite, which would cause a large drop in ductility (Schey, 1987). Similarly, for SS304, grain size refinement is also observed near the cutting area (Fig. 6(b)), which is defined as the HAZ for stainless steel in laser deburring.

3. Finite-Element Modeling

The basic interests in modeling is to determine the degree to which a laser beam which impinges onto a burr specimen will melt away the burr due to the high temperature and the resulting thermal damage due to the energy dissipated in the form of heat conduction through the material (Wei & Chiou, 1988, Wei & Ho, 1990). Figure 2(b) shows the basic concepts of modeling for a cross section of a laser deburring specimen. Also, temperature dependent mechanical properties (Peckner, 1977, Smithells, 1992) for the two specimen materials (C1045 and SS304) are used in the FEM modeling.

3.1 Analytical model

First, the analytical base for laser machining used for the numerical (FEM) model is discussed. The energy source of the model is the CO_2 laser beam. Assuming the laser beam maintains a constant Transverse Electromagnetic Mode 00 (TEM_{00}), which has the beam profile with a uniform phase front (Chryssolouris, 1990), the gaussian beam intensity distribution is described as

$$I(x, y) = a(x, y) P/R^2 \, EXP(-(x^2+y^2)/R^2) \quad (1)$$

where, $a(x, y)$ is absorptivity, R is beam radius and P is laser power

The cumulative beam energy at a given point (x, y) is the time integral of the beam intensity.

Original Workpiece(X1000)

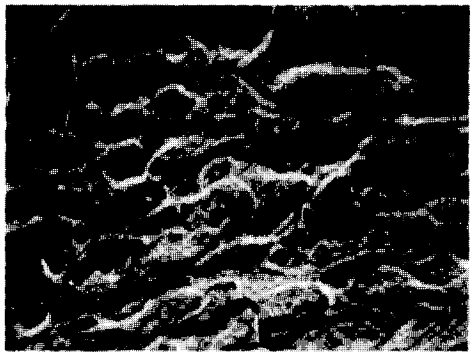

Inside the HAZ(X2000)

Fig. 6(a) Grain size refinement for carbon steel

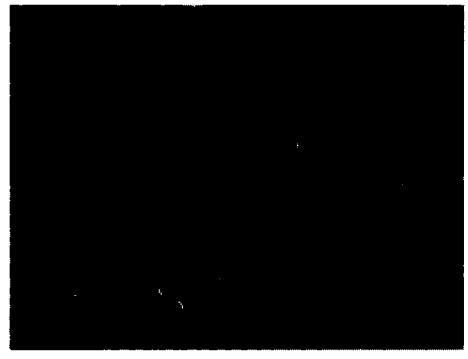

Original Workpiece(X1000)

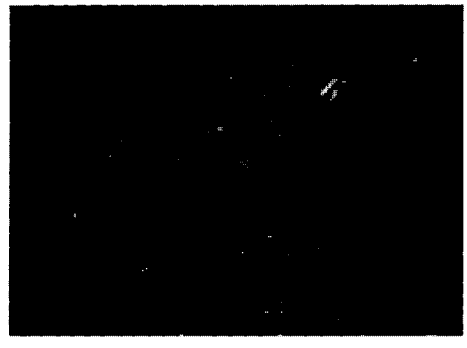

Inside the HAZ(X2000)

Fig. 6(b) Grain size refinement for stainless Steel

With a given feedrate V in the x direction, the laser beam energy can be described as

$$E_{beam}(x, y)=\int_{-\infty}^{x} I(u, y)\,dt=\int_{-\infty}^{x} I(u, y)\frac{du}{V} \quad (2)$$

The energy balance due to the effects of the laser beam, conduction and phase change in the material can be expressed as

$$E_{beam}(x, y)=E_{cond}(x, y)+E_{phase}(x, y) \quad (3)$$

As described earlier, the main heat transfer mechanism inside the workpiece during laser machining is heat conduction which can be expressed in the form of Fourier's equation:

$$\frac{\partial T}{\partial t}=\beta\nabla^2 T+V\cdot\nabla T \quad (4)$$

where, T is temperature, t is time, V is velocity vector and β is thermal diffusivity. The above equations are used either as inputs to the developed FEM code or implemented in ABAQUS, a commercial FEM software.

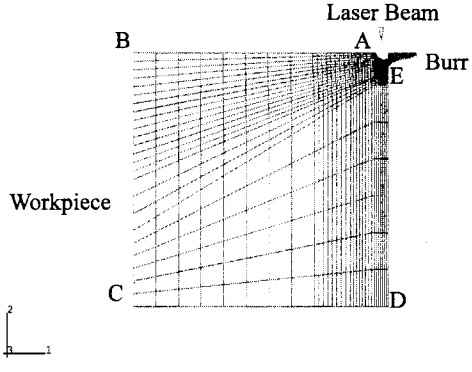

Fig. 7 FEM simulation of laser deburring

3.2 Numerical model

ABAQUS standard finite element software was used for the modeling. The current model is a two dimensional transient case, for carbon steel 1045 and stainless steel 304. For the thermo-mechanical problem, a coupled temperature-displacement analysis was used. Because this analysis is capable of performing heat transfer analysis and stress analysis together, thermal and mechanical solu-

tions can be obtained simultaneously, which provides big advantages for this particular problem. Now, the constitutive equations, energy balance and boundary conditions used in ABAQUS to simulate the problem are described.

3.2.1 Constitutive relations

3.2.1.1 Thermoelastic constitutive law

Internal energy is assumed as $U=U(T, \varepsilon^{el})$ which includes mechanical, thermal as well as coupling problems. Here, ε^{el} is elastic strain which can be expressed as.

$$\varepsilon^{el}=\varepsilon-\varepsilon^{TH}(T)-\varepsilon^{pl} \tag{5}$$

where, ε is total strain, ε^{TH} is thermal strain and ε^{pl} is plastic strain. The thermal expansion (due to thermal strain) can be expressed as

$$\varepsilon^{TH}(T)=\alpha(T)(T-T^0)-\alpha(T^I)(T^I-T^0) \tag{6}$$

where α is thermal expansion coefficient, T is the current temperature and T^0 and T^I are reference temperature and initial temperature, respectively. The constitutive relationships can be written in terms of a specific heat C(T) and true stress vector σ:

$$C(T)=\partial U/\partial T \tag{7}$$

$$\sigma=\partial U/\partial \varepsilon^{el} \tag{8}$$

Also, heat conduction is assumed to be governed by the Fourier law:

$$q=-k\ \partial T/\partial x \tag{9}$$

where k is the conductivity matrix, k=k(T); q is the heat flux and x is position.

3.2.1.2 Elastoplastic constitutive law

Assuming that the materials are isotropic elastic, isotropic hardening and follow the Von-Mises yield criterion, we have the flow rule

$$\dot{\varepsilon}^{pl}=\lambda\ \partial g/\partial \sigma \tag{10}$$

where g is the flow potential and λ is a scalar whose value is determined by the requirement to satisfy the consistency condition, and

$$\dot{\varepsilon}^{el}=\frac{\Delta}{2G}+\frac{1-2\nu}{E}\text{trace}(\sigma) \tag{11}$$

where Δ is deviatoric stress-rate tensor $\Delta=\sigma-\text{trace}(\sigma)/3$, G is shear modulus, E is Young's modulus and ν is Poisson's ratio. Therefore, strain rate decomposition can be expressed as

$$\dot{\varepsilon}=\dot{\varepsilon}^{pl}+\dot{\varepsilon}^{el}=\lambda\ \partial g/\partial\sigma+\frac{\Delta}{2G}+\frac{1-2\nu}{E}\text{trace}(\sigma) \tag{12}$$

Also, the work hardening H is given as

$$H=\frac{\partial\bar{\sigma}}{\partial\bar{\varepsilon}^{pl}} \tag{13}$$

where, $\bar{\sigma}$ is yield stress and $\bar{\varepsilon}^{pl}$ is equivalent plastic strain.

3.2.1.3 Energy balance

The basic energy balance equation is (Green & Naghdi, 1977)

$$\int_V \rho\dot{U}dV=\int_S qdS+\int_V rdV \tag{14}$$

where V is the volume of solid material, with surface S; ρ is the density; $\dot{U}$ is the material time rate of the internal energy; q is the inward heat flux per unit area of the body; and r is the heat supplied externally into the body per unit volume. In this particular problem, the external heat source will be expressed in the form of q using Eq. (9)

3.2.1.4 Boundary conditions

The boundary conditions can be specified as a prescribed temperature, T=T(x, t), prescribed surface heat flux, q=q(x, t) per area, surface convection, q=h(x, t)(T−T^0) (where h is the film coefficient) and radiation, $q=A(T^4-(T^0)^4)$. Also, the degree(s) of the freedom will be constrained at certain boundary elements.

3.2.2 Finite element approximations

In ABAQUS, the Galerkin approximation is used for spatial discretization. The coupled elements generally use a lower order interpolation for temperature than for displacement (usually parabolic variation of displacements and linear variation of temperature) in order to obtain a compatible variation of thermal and mechanical strain. As in the integration of the elastic-plastic flow, a backward difference algorithm is used for the time integration of the heat evolution, to accommodate the strongly dissipative nature of heat conduction. Also, the Newton Rapson

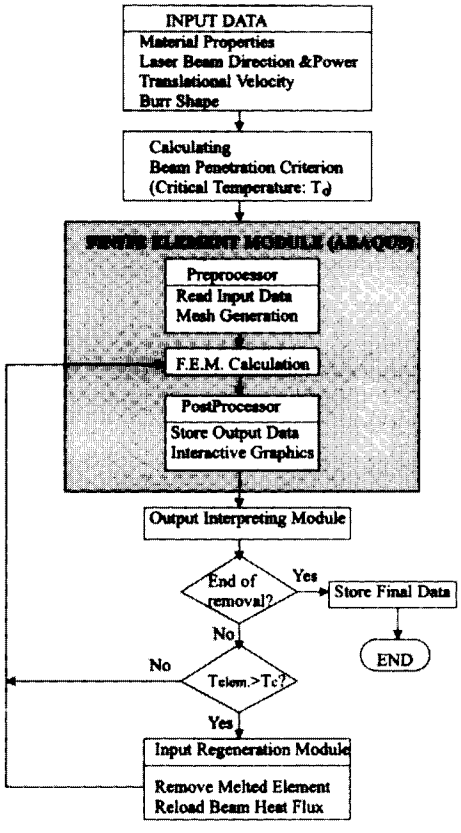

Fig. 8 Flow chart of laser deburring simulation

method is used to solve nonlinear equations for the coupled system (H. K. & S., 1989). For this two dimensional problem, a plane strain rectangular mesh with four nodes and one integration point was used.

Figure 8 shows a mesh generation for the proposed finite element model. Boundary B-C and C-D are fixed while A-B and D-E are free with surface convection. Typical side length of the workpiece model is 5mm with the burr height of 0.5mm. With input data such as (temperature-dependent) material properties, burr shape, and laser parameters to the developed code, the deburring simulation was performed. The code consists of the main FEM calculation part and an output module that determines whether further computation with a regenerated mesh is necessary and processes the calculated data (Fig. 8). An IBM RS 6000 work station was used for the FEM

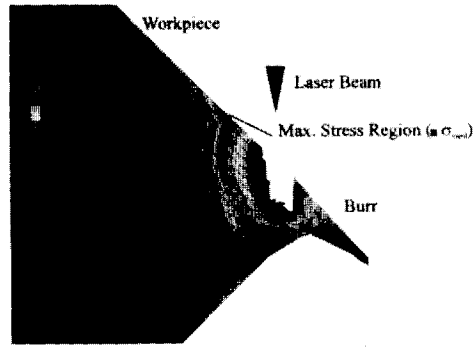

Fig. 9 Stress Distribution (Von Mises, SS304)

calculations.

4. Numerical Results

For the laser deburring problem, one of the main purposes of FEM analysis is to predict the cutting profile and the width of HAZ. For the theoretical predictions of the width of HAZ in carbon steel and stainless steel, two different criteria, yield stress and recrystallization temperature of the steel, are used.

During the laser deburring process, thermal stresses due to high temperature gradients will be induced near the cutting area. Therefore, there will be a high (compressive) stress zone adjacent to the cutting area. Figure 10 shows a magnified view of the region near the cutting area for SS304 during a laser deburring simulation. In this figure, a certain boundary next to the cutting area which experienced severe thermal stress (over the yield stress) is observed. The region within this boundary is defined as the HAZ based on the yield criterion. Also, if a certain area of the material experiences a higher temperature than the recrystallization temperature, it is defined as part of the HAZ by the temperature criterion. Figure 10 shows the temperature distribution right after deburring for carbon steel 1045. Likewise, by tracing the temperature and stress history of each element during the simulation, then checking to see if the values exceed these criteria, the HAZ width can be predicted.

For the temperature criterion (in FEM) recrystallization temperature was used to determine the HAZ size. As grain size refinement, carbide pre-

cipitation, etc. during laser machining are directly related to the steep rise of temperature, this criterion seems reasonable. However, it has several problems in applying to the FEM simulation. First, to set an effective recrystallization temperature in the simulation is difficult. Sheng et al. (1995) used only the temperature criterion to determine the HAZ size after laser machining using FEM. But, the size of HAZ was always underestimated compared to the experimental results. This is partly due to the fact that laser heat flux was assumed as Gaussian heat flux. High temperatures are concentrated at the lower portion of the laser melting kerf and the heat conduction to the side direction (-x direction in Fig. 2(b)) was not exactly represented at the cutting (deburring) stage, when the heating source moves down (y direction) very fast. This is the second problem.

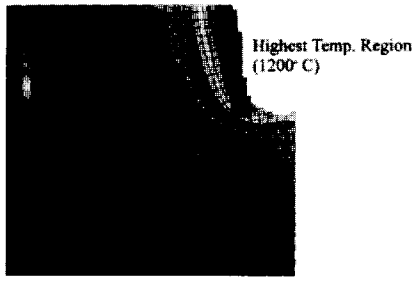

Fig. 10 Temperature distribution (Laser off, C1045)

As time evolves in the simulation, the transient

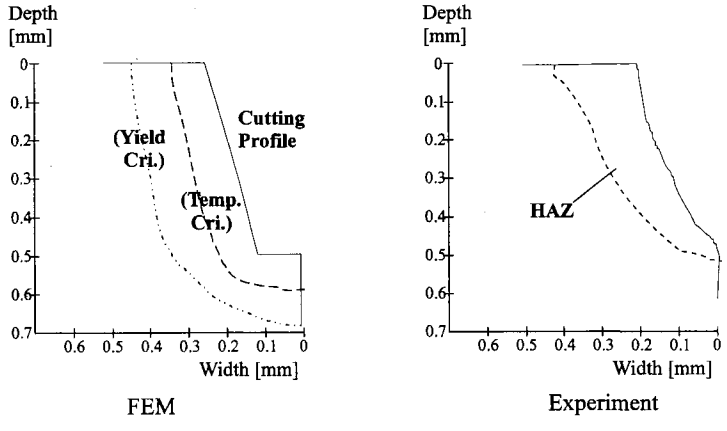

(a) C1045 (Power=300W, Feedrate=1mm/sec., Burr th.=0.25mm)

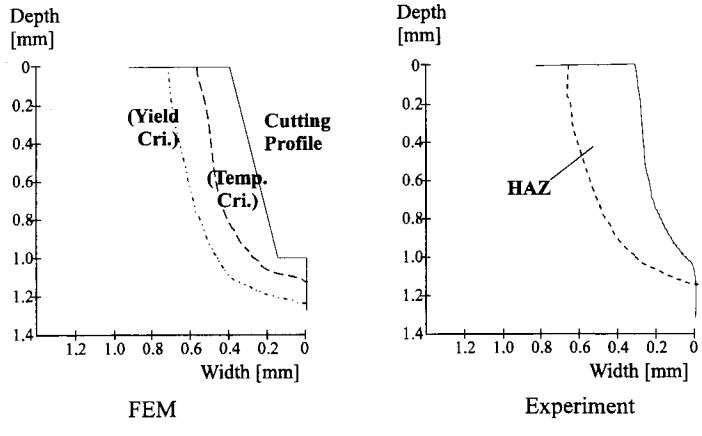

(b) SS304 (Power=500W, Feedrate=1mm/sec., Burr th.=0.50mm)

Fig. 11 HAZ prediction using FEM

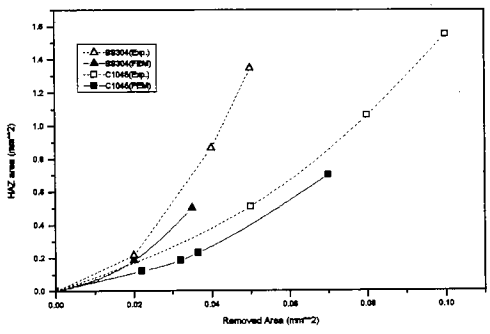

Fig. 12 HAZ area (Laser Power=300W)

heat conduction process results in thermo-plastic softening of the material which induces plastic flow. This is the basis of stress criterion, which represents the bulk phenomena due to the heat, regardless of direction, as well as residual stress due to the melting-solidification process. Moreover, compared to the experimental results, the prediction using stress criterion gives closer agreement, which supports the above statement.

Figure 12 shows the HAZ prediction using the yield stress criterion. In Fig. 12, the HAZ areas (from both the experiment and the FEM analysis (yield criterion)) are plotted against the removed material area. In both the SS304 and carbon steel cases, the results show good agreement between simulation and experiment.

5. Conclusion

A thermal procedure, laser machining, has been proposed as a deburring technique for precision components. Using experimental tests as well as numerical simulations (FEM), the process has been analyzed and evaluated for practicality in automated deburring.

From the SEM investigation of the experimental workpieces, it has been found that laser deburring provides reasonably accurate dimension and minimal size of HAZ, thus minimal material property changes. Also, the FEM analysis can effectively predict the important aspects of laser deburring such as cutting profiles, stress distributions near the cutting area and HAZ. It also shows good agreement with experimental results.

Combined with an effective process control and appropriate sensing techniques, laser deburring could be a viable approach for automated precision deburring. Furthermore, for special applications such as burrs around intersecting holes, a situation in which no mechanical deburring tools are effective, laser deburring would have an advantage over conventional deburring techniques.

References

Alwerfalli, D. R., 1975, "Deburring Metal Parts," *American Machinist*, pp. 55~62

American Welding Society, 1991, *Welding Hand Book*, 8th edition, Vol. 2.

Cai, L., 1996, "Model Based Process Planning of a Laser Cutting," *Ph. D dissertation, U. C. Berkeley*.

Chryssolouris, George, 1990, "Laser Machining," Springer-Verlag, New York.

Cline, H. E. and Anthoy, T. R., 1977, "Heat Treating and Melting of Material with a Scanning Laser or Electron Beam," *Journal of Applied Physics*, Vol. 48, N9.

De Litzia, A., 1986, "Mechanical Deburring with Centrifugal Blast Equipment," *Advancement in Surface Treatment Technology*, Vol. 2, pp. 241~254.

Gillespie, L. K., 1979, "Deburring Precision Miniature Parts," *Precision Engineering*, Vol. 1, N4, pp. 189~198

Glass, J. M., et al., 1977, "Heat Transfer in Metallic Glasses during Laser Cutting," *Heat Transfer in Manufacturing and Materials Processing*, HTD, Vol., 13, pp. 31~38.

Green, A. E. and Naghdi, P. M., 1977, "A General Theory of an Elastic-Plastic Continuum," *Archives of Rational Mechanics and Analysis*, Vol. 17.

Geiger, M. et al., 1988, "Laser Cutting of Steel Sheets," *Laser Assisted Processing, SPIE*, Vol. 1022, pp. 20~33.